

# Towards the One Learning Algorithm Hypothesis: A System-theoretic Approach

Christos N. Mavridis, *Member, IEEE*, and John S. Baras, *Life Fellow, IEEE*

**Abstract**—The existence of a universal learning architecture in human cognition is a widely spread conjecture supported by experimental findings from neuroscience. While no low-level implementation can be specified yet, an abstract outline of human perception and learning is believed to entail three basic properties: (a) hierarchical attention and processing, (b) memory-based knowledge representation, and (c) progressive learning and knowledge compaction. We approach the design of such a learning architecture from a system-theoretic viewpoint, developing a closed-loop system with three main components: (i) a multi-resolution analysis pre-processor, (ii) a group-invariant feature extractor, and (iii) a progressive knowledge-based learning module. Multi-resolution feedback loops are used for learning, i.e., for adapting the system parameters to online observations. To design (i) and (ii), we build upon the established theory of wavelet-based multi-resolution analysis and the properties of group convolution operators. Regarding (iii), we introduce a novel learning algorithm that constructs progressively growing knowledge representations in multiple resolutions. The proposed algorithm is an extension of the Online Deterministic Annealing (ODA) algorithm which can be viewed as a competitive-learning neural network where the neurons represent codevectors in the data space and the training rule is based on annealing optimization, solved using gradient-free stochastic approximation. ODA has inherent robustness and regularization properties and provides a means to progressively increase the complexity of the learning model i.e. the number of the neurons, as needed, through an intuitive bifurcation phenomenon. The proposed multi-resolution approach is hierarchical, progressive, knowledge-based, and interpretable, allowing the localization of the error-prone regions of the data space. We illustrate the properties of the proposed architecture in the context of the state-of-the-art learning algorithms and deep learning methods.

**Index Terms**—Hierarchical Learning, Progressive Learning, Annealing Optimization, Online Deterministic Annealing, Multi-resolution Analysis, One Learning Algorithm Hypothesis.

## I. INTRODUCTION

**L**EARNING from data samples has become an important component in the advancement of numerous research fields including artificial intelligence, computational physics, biology and control systems. While virtually all learning problems can be formulated as constrained stochastic optimization problems, the optimization methods can be intractable due to the nature of the problems and the constraints originating from the model assumptions. For this reason, some of the most impactful breakthroughs in machine learning research have

The authors are with the Department of Electrical and Computer Engineering and the Institute for Systems Research, University of Maryland, College Park, USA. emails: {mavridis, baras}@umd.edu.

Research partially supported by the Defense Advanced Research Projects Agency (DARPA) under Agreement No. HR00111990027, by ONR grant N00014-17-1-2622, and by a grant from Northrop Grumman Corporation.

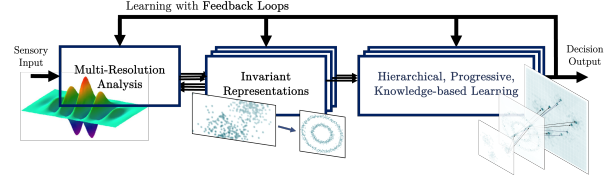


Fig. 1: Abstract system-theoretic block diagram of a “universal learning architecture” in human cognition.

been a result of selecting appropriately structured learning models that can be trained efficiently using existing optimization methods [1].

In search for appropriate learning models and inspired by established experimental findings from neuroscience [2], [3], a widely spread conjecture has been formed regarding the existence of a universal learning model in human cognition. While no observations can yet lead to the specifics of the implementation of such an architecture, at an abstract level it is believed that human perception, cognition, and learning, are based on three main properties: (a) hierarchical attention and information processing [3]–[8], (b) memory-based knowledge representation [9], and (c) progressive learning and knowledge compaction [10], [11].

Deep learning methods, currently dominating the field of machine learning due to their performance in numerous applications, have made progress towards this direction, especially regarding the hierarchical properties (a). They attempt to learn feature representations from data, using biologically-inspired models in artificial neural networks that mimic the low-level computational architecture of the human brain units [11]–[14]. They provide task-specific end-to-end learning algorithms implemented by a non-von Neumann computational architecture that does not discriminate between computational and memory units. As a result, however, they do not provide a framework for memory representation and knowledge compaction as in (b) and (c).

On the other hand, it is understood that artificial intelligence systems need not mimic the low-level architecture of the brain cells, but rather get inspirations from abstract properties of human intelligence [15]. This becomes especially important when considering that adopting black-box deep neural network architectures results in using overly complex models of a great many parameters in the expense of time, energy, data, memory and computational resources [16], [17]. Even in the applications when complexity is not an issue, the lack of interpretability and mathematical understanding, and the vulnerability to small perturbations and adversarial attacks

[18]–[20], has led to an emerging hesitation in the use of deep learning models outside common benchmark datasets [21], [22], and, especially, in security critical applications. These models are hard to analyze with current mathematical tools, hard to train with current optimization methods, and their design relies solely in experimental heuristics. As a result, researchers have been trying to answer questions about their approximation power, the dynamics and convergence of optimization, the properties of the intrinsically generated representations, and the phenomena of overfitting, regularization, and overparameterization, in an attempt to understand the conditions under which deep learning methods work as expected [10], [23]–[26].

To this end, we approach the design of a “universal learning architecture” [27], [28] from a system-theoretic viewpoint, based on the aforementioned architectural abstractions of the processing system of the auditory and visual cortex of the human [3]–[8]. The architecture consists of a closed-loop system with three main components:

- (i) a hierarchical signal decomposition unit based on multi-resolution wavelet analysis [24],
- (ii) a feature extraction module that, in combination with (i), estimates group-invariant representations in multiple resolutions, and
- (iii) a hierarchical, progressive, robust, and interpretable learning model for supervised and unsupervised learning that is able to represent and progressively compact accumulated knowledge.

Multi-resolution feedback loops are used for adaptive estimation of the optimal parameters for (i), (ii), and (iii). An abstract block diagram is depicted in Fig. 1.

Regarding the subsystems (i) and (ii), we follow the established theory of wavelet decomposition to build a multi-resolution representation of the input. Wavelet decomposition is based on a cascade of convolution and downsampling operators. Convolutions create translation equivariant representations which are stable to deformations, and can be generalized to carry these properties to any known compact Lie group [29]. Downsampling, on the other hand, constitutes an averaging operation that creates local invariance, and can be viewed as a pooling operation. Finally, creating a hierarchical cascade of convolution operations followed by non-linear mappings (subsystem (ii)) and averaging functions, has been shown to construct multi-scale group-invariant representations [24].

Regarding (iii), we build upon the Online Deterministic Annealing (ODA) algorithm [30], a novel learning algorithm that constructs progressively growing knowledge representations. ODA can be formulated as a series of soft-clustering optimization problems

$$\min_M F_T(M) := D(M) - TH(M),$$

parameterized by a temperature coefficient  $T$ . Here  $D$  is the average distortion  $D(M) := \mathbb{E}[\sum_i p(\mu_i|X)d(X, \mu_i)]$  measured by  $d$ , the proximity measure that defines the similarity between the random input  $X$  and a codevector  $\mu_i$  with appropriately defined association probabilities  $p(\mu_i|X)$ .  $H$  represents the Shannon entropy that characterizes the “purity”

of the clusters induced by the codevectors, and  $T$  acts as a Lagrange multiplier controlling the trade-off between minimizing the distortion  $D$  and maximizing the entropy  $H$ . The codevectors can be viewed as a set of neurons, the weights of which live in the data space itself. The representation of the input in terms of memorized exemplars is an intuitive approach which parallels similar concepts from cognitive psychology and neuroscience and induces interpretability. Moreover, it resembles vector quantization algorithms, which have shown impressive robustness against adversarial attacks, suggesting suitability in security critical applications [31]. By successively solving the optimization problems  $\min_M F_T(M)$  for decreasing values of  $T$ , the model undergoes a series of phase transitions when the cardinality of the set of codevectors  $M$  increases, according to an intuitive bifurcation phenomenon. This resembles an annealing process [32] that introduces inherent robustness and regularization properties. The optimization problems are solved using gradient-free stochastic approximation [33], provided that the proximity measure  $d$  belongs to the family of Bregman divergences: information-theoretic dissimilarity measures (including the widely used Kullback-Leibler divergence) that have been shown to play an important role in learning applications [34], [35].

Finally, to construct a hierarchical multi-resolution learning approach for (iii), we develop a tree-structured ODA learning algorithm. Traditional tree-structured vector quantization algorithms partition the data space by building a labeled binary tree using ad-hoc splitting criteria. This yields a faster, yet suboptimal solution to the original problem. In contrast, we train each layer of the tree with the ODA algorithm that progressively adjusts the number of codevectors-children for each node according to the annealing optimization process. Moreover, to make use of multiple-resolutions, we extend this approach having each layer trained using progressively more detailed representations according to the multi-resolution analysis of (i) and (ii). As will be shown, the combination of the convolution-based multi-resolution features with the proposed tree-structured multi-layer neural network resembles the structure of Deep Convolutional Networks [11] and Scattering Convolutional Networks [36], and provides a general system-theoretic framework for progressive, hierarchical, interpretable, and knowledge-based learning.

## II. HIERARCHICAL AND INVARIANT REPRESENTATIONS

To understand how deep learning models work, it is important to mathematically characterize the properties of the internally learned representations [13], [37]–[39] and its inductive bias, i.e., the class of tasks for which they are predesigned to perform well. As an example, in computer vision tasks, geometric stability has been shown to play an important role and can be measured in terms of invariance to translations and stability to local deformations, as will be explained later. Deep convolutional neural networks have been shown to provide this geometrical stability [25] by following a compositional approach with a hierarchically structured model [11], [40]. The structure is mainly composed by successive operations of a linear operator (or linear filter, e.g., convolutional layers),

a nonlinear mapping (often a rectifying function, e.g., ReLu), and a down-sampling step (e.g., max-pooling), which produces the input for the next stage of the architecture [24], [36], [41]. This approach seems to reflect neuro-scientific findings [4], [40], [42], and is also reminiscent of the multi-resolution representations produced by the extensively studied wavelet transform. The wavelet transform [43], as well as extensions including the wavelet packets [44], offer a solid mathematical tool to understand the properties of the multi-resolution representation of a signal. As a result, wavelets have been already used to study the mathematics of deep learning, with the scattering transform [24], [36] having been shown to preserve the aforementioned geometric stability properties, hinting that convolution filters need not be learned from data, but can be defined a priori with respect to the properties of the task at hand.

In this section, we briefly review the mathematics of the wavelet and wavelet packet transform and show how they can be used to build multi-resolution locally invariant representations with respect to compact Lie groups.

#### A. Wavelet-based Multi-Resolution Analysis

Consider a measurable signal  $f(t)$  with finite energy, i.e.,  $f(t) \in L^2(\mathbb{R}^n)$ . We will focus in one-dimensional signals ( $n = 1$ ) for simplicity of notation, although the analysis can be generalized for any  $n > 0$ . The continuous wavelet transform of  $f$  corresponds to the set of coefficients of the atoms of a redundant dictionary of time-scale images (in  $(u, s)$ ):

$$\left\{ \psi_{u,s}(t) = \frac{1}{\sqrt{s}} \psi\left(\frac{t-u}{s}\right) \right\}_{u \in \mathbb{R}, s > 0} \quad (1)$$

where  $\psi \in L^2(\mathbb{R})$  has zero average, i.e.,  $\int_{-\infty}^{\infty} \psi(t) dt = 0$ , and is called the mother wavelet. In many useful cases, such as in directional wavelets for 2D images, the mother wavelets are defined such that the redundant dictionaries constitute a complete and stable signal representation, called a frame [44]. For simplicity of notation, we will focus on orthonormal (Riesz) bases which remove all redundancy and define stable representations. A wavelet orthonormal basis is obtained by scaling a wavelet  $\psi$  with a dyadic scale  $s = 2^j$  and translating it by  $u = 2^j n$ :

$$\left\{ \psi_{j,n}(t) = \frac{1}{\sqrt{2^j}} \psi\left(\frac{t-2^j n}{2^j}\right) \right\}_{(j,n) \in \mathbb{Z}^2} \quad (2)$$

The simplest orthonormal basis can be constructed using the piecewise constant Haar wavelets, but regular wavelets of compact support can form an orthonormal basis as well [44]. The signal  $f$  can be expressed in the wavelet bases as:

$$f = \sum_{j=-\infty}^{\infty} \sum_{n=-\infty}^{\infty} c_{j,n} \psi_{j,n} \quad (3)$$

where  $c_{j,n} = \langle f, \psi_{j,n} \rangle$ . Moreover,  $f$  can be expressed as a direct sum:

$$f = \sum_{j > J} \sum_{n=-\infty}^{\infty} c_{j,n} \psi_{j,n} + \sum_{j \leq J} \sum_{n=-\infty}^{\infty} c_{j,n} \psi_{j,n} \quad (4)$$

$$= \sum_{n=-\infty}^{\infty} a_{J,n} \phi_{J,n} + \sum_{j \leq J} \sum_{n=-\infty}^{\infty} c_{j,n} \psi_{j,n} \quad (5)$$

where  $\phi_{j,n}$  is called the scaling function and is defined similar to (2) according to a mother scaling function  $\phi$ . The set  $\{\phi_{J,n}\}$  is an orthonormal basis of the subspace  $V_J \subset L^2(\mathbb{R})$  which corresponds to the approximation of  $L^2(\mathbb{R})$  at resolution  $J$ , and has the following properties:

- $V_j \subset V_{j-1}, \forall j \in \mathbb{Z}$ ,
- $\cup_{j=-\infty}^{\infty} V_j$  is dense in  $L^2(\mathbb{R})$  with  $\cap_{j=-\infty}^{\infty} V_j = \{0\}$ ,
- $f(t) \in V_j \Leftrightarrow f(2t) \in V_{j-1}, \forall j \in \mathbb{Z}$ , and
- $f(t) \in V_j \implies f(t - 2^j k) \in V_j, \forall k \in \mathbb{Z}$ .

It is easy to see that the sum  $\sum_{n=-\infty}^{\infty} c_{j,n} \psi_{j,n}$  is an orthonormal basis for the subspace  $W_j$  for which  $V_j \oplus W_j = V_{j-1}$  and  $V_J = \oplus_{j > J} W_j$ . In other words, the additional information lost in the approximation  $V_J$  at resolution  $2^J$  is contained in the subspace  $W_J$ .

In practice, a physical measurement device can only measure a signal at a finite resolution, denoted by  $j = 0$ . Then the coefficients  $\{c_{j,n}\}_{j \in \mathbb{N}}$  and  $\{a_{j,n}\}_{j \in \mathbb{N}}$  define the multi-resolution representation of the wavelet transform. Moreover, the coefficients

$$\begin{aligned} c_{j,n} &= \langle f, \psi_{j,n} \rangle = \int_{-\infty}^{\infty} f(t) \psi_{j,n}(t) dt \\ a_{j,n} &= \langle f, \phi_{j,n} \rangle = \int_{-\infty}^{\infty} f(t) \phi_{j,n}(t) dt \end{aligned} \quad (6)$$

can also be written as:

$$\begin{aligned} \langle f, \psi_{j,n} \rangle &= (f * \psi_{2^j})(t)|_{t=2^j n} := W_j f(t)|_{t=2^j n} \\ \langle f, \phi_{j,n} \rangle &= (f * \phi_{2^j})(t)|_{t=2^j n} \end{aligned} \quad (7)$$

where  $\psi_{2^j}(x) = 2^{-j/2} \psi(-2^{-j}x)$ ,  $\phi_{2^j}(x) = 2^{-j/2} \phi(-2^{-j}x)$ , and  $(f * g)(x) = \int_{-\infty}^{\infty} f(u)g(x-u)du$  is the convolution operation. Taking into account that  $\psi_{2^j}, \phi_{2^j} \in V_{j-1}$ , the coefficients can be computed by:

$$\begin{aligned} \langle f, \psi_{j,n} \rangle &= (g * \langle f, \phi_{2^{j-1}} \rangle)(t)|_{t=2^n} \\ \langle f, \phi_{j,n} \rangle &= (h * \langle f, \phi_{2^{j-1}} \rangle)(t)|_{t=2^n} \end{aligned} \quad (8)$$

Equation (8) reveals that the wavelet coefficients  $\langle f, \psi_{j,n} \rangle$ ,  $\langle f, \phi_{j,n} \rangle$  can be computed by hierarchical filtering with appropriately defined filters associated with the mother wavelet  $\psi$ , followed by a uniform downsampling by a factor of 2. In particular,  $h$  is a low-pass filter and  $g$  is a high-pass filter. They depend on  $\phi$  and  $\psi$ , and define a pair of quadrature mirror filters, an observation that has led to the fast filter-bank implementation of the wavelet transform and its association with multi-resolution analysis [43].

#### B. Wavelets, Translation Invariance, and Stability to Deformations

As shown above, the computation of the multi-resolution wavelet representation of a signal consists of successive oper-

ations of a linear convolution operator, followed by a down-sampling step. This structure is similar to deep convolutional neural networks, and has been very successful in multiple applications, especially in sound and image recognition, where translation invariance and stability to small deformations are important properties of the representation [24]. The translation group is a Lie group of operators  $\{T_c\}_{c \in \mathbb{R}}$  such that  $T_c f(t) = f(t-c)$ , while the group of deformations  $D_\tau$  can be written as  $D_\tau f(t) = f(t-\tau(t))$ , where the local function  $\tau$  depends on  $t$  and thus deforms the image. A representation  $\Phi : L^2(\mathbb{R} \rightarrow H$ , where  $H$  is a Hilbert space, is said to be invariant with respect to  $T_c$  if  $\Phi(T_c f) = \Phi(f)$ . The wavelet transform (eq. (7)) is based on the convolution operation, and is therefore translation covariant (or equivariant), i.e., it commutes with the translation operator and satisfies the relation  $W_j(T_c f) = T_c W_j(f)$ . At the same time, the wavelet transform, is stable to small deformations, which is a very important property that can be expressed as a Lipschitz continuity condition:

$$\|W_j(D_\tau f) - W_j(f)\|_2 \leq C \|f\|_2 \sup_t |\nabla \tau(t)| \quad (9)$$

where  $\|f\|_2 = \int |f(t)|^2 dt$  is the  $L^2(\mathbb{R})$  norm, and  $|\nabla \tau(t)|$  is a measure of the deformation amplitude (it is assumed that  $|\nabla \tau(t)| < 1$ , which makes the small deformation an invertible transformation [36]).

**Remark 1.** *We note that, in the control theory and signal processing communities, convolutions are associated with systems described by the term 'linear time-invariant'. To avoid confusion, with the terminology used here, these systems are considered linear covariant (or equivariant) operators with respect to translation in time.*

To induce invariance with respect to translation, it is sufficient to integrate (average) a translation-covariant representation over the translation group. That is to say that the integral  $\int W_j f(c) dc$  is translation invariant. However, it turns out to be the trivial invariant  $\int_{-\infty}^{\infty} W_j f(t-c) dc = 0$ , since, by definition,  $\int_{-\infty}^{\infty} \psi(t) dt = 0$ . Therefore, it is necessary to insert a non-linear operation between the wavelet transform and the integration [36]. It has been shown that a point-wise and stable non-linear operator  $\rho$  (for stability:  $\|\rho f\| \leq \|f\|$  and  $\|\rho f - \rho g\| \leq \|f - g\|$ ), that also commutes with the translation (and the deformation) group, is the  $L^1(\mathbb{R})$  norm:  $\|f\|_1 = \int |f(t)| dt$ , which acts as a rectifying function, similar to the ReLU function in deep convolutional neural networks. The choice  $\rho = \|\cdot\|_1$  also preserves the deformation stability properties of the wavelet transform.

The cascade of the wavelet transform, the non-linear operation, and the averaging integral, results in the representation  $\int \rho W_j(f)(t) dt$ , in every resolution  $j$ . However, global invariance is not always desired. In contrast, it is often better to compute locally invariant representations for translations up to a scale  $2^J$  for some index  $J$ . This can be obtained by substituting the integral by a convolution with a low-pass filter localized in a spatial window scaled at  $2^J$ . The result is a representation that belongs to  $V_J$ , and, in particular the projection of  $\rho W_j(f)$  to  $V_J$ , for  $J \geq j$ , which can be computed by the pyramid of filters of the wavelet transform, as explained above.

Moreover, during the computation of the wavelet transform, the information lost in averaging (projecting to  $V_J$ ) is kept in the coefficients  $\{c_{j,n}\}_{j < J}$  of the wavelet transform. This information can be used to build new invariant features by applying the wavelet transform again, creating a deep scattering network introduced by Bruna in [36]. The implementation of the scattering transform is based on a complex-valued convolutional neural network whose filters are fixed wavelets and  $\rho$  is a complex modulus operator as described above [45]. We note that the features of the scattering transform do not belong to the subspaces  $\{V_j, j \in \mathbb{N}\}$  that define the classical wavelet hierarchy. However, they define a multi-level hierarchy of successively more detailed information that can be used in a similar way.

### C. Building Invariance to compact Lie Groups

The invariance properties discussed above can be generalized to the action of arbitrary compact Lie groups, such as a rotation and translation group [29]. Let  $G$  be a compact Lie group and  $L^2(G)$  be the space of measurable functions  $f(r)$  such that  $\|f\|^2 = \int_G |f(r)|^2 dr < \infty$ , where  $dr$  is the Haar measure of  $G$ . The left action of  $g \in G$  on  $f \in L^2(G)$  is defined by  $L_g f(r) = f(g^{-1}r)$ . As a special case, the action of the translation group  $T_c f(t) = f(t-c)$  translates the function  $f$  to the right by  $c$ , with  $g^{-1} = -c$  translating the argument of  $f$  to the left by  $c$ . Similar to the usual convolution  $(f * h)(x) = \int_{-\infty}^{\infty} f(u)h(x-u)du$  that defines a linear translation covariant operator, convolutions on a group appear naturally as linear operators covariant to the action of a group:

$$(f * h)(x) = \int_G f(g)h(g^{-1}x)dr \quad (10)$$

where  $dr$  is the Haar measure of  $G$ . As a result, an invariant representation relatively to the action of a compact Lie group, can be computed by averaging over covariant representations created by group convolution with appropriately defined wavelets, similar to the methodology explained above.

### D. Multi-resolution Feedback Loops

The methodology explained in Section II-C can be used to build invariant features with respect to a known compact Lie Group. In the case of image and sound recognition, it has been shown that local invariance with respect to the groups of spatial translation and rotation is sufficient [24]. In other words, the groups with respect to which we design the wavelet-based features described above, are known a priori. In general, such information may not be known, and may need to be estimated from the data. This is the purpose of the multi-resolution feedback loops presented in Fig. 1, and specifically, the first set of feedback loops shown in Fig. 3(a). The wavelet transform used can be generalized to a redundant hierarchical dictionary, as well, the basis of which can be estimated again from data via the same feedback loops. In the case of a wavelet transform this reduces to estimating the mother wavelet [46]. To estimate different non-linear functions  $\rho$ , the second set of feedback loops can also be used. Therefore, the multi-resolution feedback loops make the proposed approach a



general framework for task-agnostic learning. Estimating this non-linear mapping or the mother wavelet from data is beyond the scope of this paper.

### III. ONLINE DETERMINISTIC ANNEALING FOR UNSUPERVISED AND SUPERVISED LEARNING

To build a progressive learning algorithm with the properties mentioned above, we will start our analysis with unsupervised learning, which can provide valuable insights into the nature of the dataset at hand, and it plays an important role in the context of visualization. Central to unsupervised learning is the representation of data in a vector space by typical representatives which is implemented with vector quantization variants [47]. Given a random variable  $X : \Omega \rightarrow S$  defined in the probability space  $(\Omega, \mathcal{F}, \mathbb{P})$ , a quantizer  $Q : S \rightarrow S$  is defined such that  $Q(X) = \sum_{h=1}^K \mu_h \mathbb{1}_{[X \in S_h]}$ , where  $V := \{S_h\}_{h=1}^K$  forms a partition of  $S$  and  $M := \{\mu_h\}_{h=1}^K$  represents a set of codevectors such that  $\mu_h \in \text{ri}(S_h)$ ,  $h \in \{1, \dots, K\}$ . Given a dissimilarity measure  $d : S \times \text{ri}(S) \rightarrow [0, \infty)$  one seeks the optimal  $M, V$  in terms of minimum average distortion:

$$\min_{M, V} D(Q) := \mathbb{E}[d(X, Q(X))] \quad (11)$$

Vector quantization algorithms assume that  $Q$  is a deterministic function of  $X$  and are proven to converge to locally optimal configurations even when formulated as online learning algorithms [47]. However, their convergence properties and final configuration depend heavily on two design parameters: (a) the number of clusters (neurons), and (b) their initial configuration. To deal with this phenomenon, the Online Deterministic Annealing approach [30] makes use of a probabilistic framework, where input vectors are assigned to clusters in probability, thus dropping the assumption that  $Q$  is a deterministic function of  $X$ . For the randomized partition, the expected distortion becomes:

$$D = \mathbb{E}[d_\phi(X, Q)] = \mathbb{E}[\mathbb{E}[d_\phi(X, Q)|X]]$$

The central idea of deterministic annealing is to seek the distribution that minimizes  $D$  subject to a specified level of randomness, measured by the Shannon entropy

$$H(X, M) = H(X) - \mathbb{E}[\mathbb{E}[\log p(Q|X)|X]]$$

with  $p(\mu|x)$  representing the association probability relating the input vector  $x$  with the codevector  $\mu$ . This is essentially a realization of the Jaynes's maximum entropy principle [48]. The resulting multi-objective optimization is conveniently formulated as the minimization of the Lagrangian

$$F = D - TH \quad (12)$$

where  $T$  is the temperature parameter that acts as a Lagrange multiplier. Clearly, (12) represents the scalarization method for trade-off analysis between two performance metrics. For large values of  $T$  we maximize the entropy, and, as  $T$  is lowered, we essentially transition from one Pareto point to another in a naturally occurring direction that resembles an annealing process. In this regard, the entropy  $H$ , which is closely related to the "purity" of the clusters, acts as a regularization term which is given progressively less weight

as  $T$  decreases. As is the case in vector quantization, one minimizes  $F$  via a coordinate block optimization algorithm. Minimizing  $F$  with respect to the association probabilities  $p(\mu|x)$  is straightforward and yields the Gibbs distribution

$$p(\mu|x) = \frac{e^{-\frac{d(x, \mu)}{T}}}{\sum_{\mu} e^{-\frac{d(x, \mu)}{T}}} \quad (13)$$

while, in order to minimize  $F$  with respect to the codevector locations  $\mu$  we set the gradients to zero

$$\frac{d}{d\mu} D = 0 \implies \frac{d}{d\mu} \mathbb{E}[\mathbb{E}[d(X, \mu)|X]] = 0 \quad (14)$$

#### A. Bifurcation Phenomena

Adding to the physical analogy, it is significant that, as the temperature is lowered, the system undergoes a sequence of "phase transitions", which consists of natural cluster splits where the cardinality of the codebook (number of prototypes) increases. This is a bifurcation phenomenon that provides a useful tool for controlling the size of the model relating it to the scale of the solution. At very high temperature ( $T \rightarrow \infty$ ) the optimization yields uniform association probabilities  $p(\mu|x) = 1/K$ , and all the codevectors are located at the same point. This is true regardless of the number of codevectors available. We refer to the number of different codevectors resulting from the optimization process as *effective codevectors*. These define the cardinality of the codebook, which changes as we lower the temperature. The bifurcation occurs when the solution above a critical temperature  $T_c$  is no longer the minimum of the free energy  $F$  for  $T < T_c$ . A set of coincident codevectors then splits into separate subsets. These critical temperatures  $T_c$  can be traced when the Hessian of  $F$  loses its positive definite property, and are, in some cases, computable (see Theorem 1 in [32]). In other words, an algorithmic implementation needs only as many codevectors as the number of effective codevectors, which depends only on the temperature parameter, i.e. the Lagrange multiplier of the multi-objective minimization problem in (12). As shown in [30], we can detect the bifurcation points by maintaining and perturbing pairs of codevectors at each effective cluster so that they separate only when a critical temperature is reached.

#### B. Bregman Divergences as Dissimilarity Measures

The proximity measure  $d$  need not be a metric, and can be generalized to more general dissimilarity measures inspired by information theory and statistical analysis. In particular, the family of Bregman divergences, which includes the widely used Kullback-Leibler divergence, can offer numerous advantages in learning applications compared to the Euclidean distance alone [34]. Notably, in the case of deterministic annealing, Bregman divergences play an even more important role, since we can show that, if  $d$  is a Bregman divergence, the solution to the second optimization step (14) can be analytically computed in a convenient centroid form [30]:

$$\mu^* = \mathbb{E}[X|\mu] \quad (15)$$

### C. The online learning rule

In an offline approach, the approximation of the conditional expectation  $\mathbb{E}[X|\mu]$  is computed by the sample mean of the data points weighted by their association probabilities  $p(\mu|x)$ . To define an online training rule for the deterministic annealing framework, we formulate a stochastic approximation algorithm to recursively estimate  $\mathbb{E}[X|\mu]$  directly. As a direct consequence of Theorem 4 in [30], the following corollary provides an online learning rule that solves the optimization problem of the deterministic annealing algorithm.

**Corollary 0.1.** *The online training rule*

$$\begin{cases} \rho_i(n+1) &= \rho_i(n) + \beta(n) [\hat{p}(\mu_i|x_n) - \rho_i(n)] \\ \sigma_i(n+1) &= \sigma_i(n) + \beta(n) [x_n \hat{p}(\mu_i|x_n) - \sigma_i(n)] \end{cases} \quad (16)$$

where  $\sum_n \beta(n) = \infty$ ,  $\sum_n \beta^2(n) < \infty$ , and the quantities  $\hat{p}(\mu_i|x_n)$  and  $\mu_i(n)$  are recursively updated as follows:

$$\mu_i(n) = \frac{\sigma_i(n)}{\rho_i(n)}, \quad \hat{p}(\mu_i|x_n) = \frac{\rho_i(n) e^{-\frac{d(x_n, \mu_i(n))}{T}}}{\sum_i \rho_i(n) e^{-\frac{d(x_n, \mu_i(n))}{T}}} \quad (17)$$

converges almost surely to a solution of the block optimization (13), (15).

The learning rule (16), (17) is a stochastic approximation algorithm [33].

### D. Online Deterministic Annealing for Supervised Learning

We can extend the proposed learning algorithm to be used for classification as well. For the classification problem, a pair of random variables  $\{X, c\} \in S \times \{0, 1\}$  defined in a probability space  $(\Omega, \mathcal{F}, \mathbb{P})$ , is observed with  $c$  representing the class of  $X$  and  $S \subseteq \mathbb{R}^d$ . Let  $M := \{\mu_h\}_{h=1}^K$ , where  $\mu_h \in \text{ri}(S_h)$  represent codevectors, and define the set  $C_\mu := \{c_{\mu_h}\}_{h=1}^K$ , such that  $c_{\mu_h} \in \{0, 1\}$  represents the class of  $\mu_h$  for all  $h \in \{1, \dots, K\}$ . The quantizer  $Q^c : S \rightarrow \{0, 1\}$  is defined such that  $Q^c(X) = \sum_{h=1}^K c_{\mu_h} \mathbb{1}_{[X \in S_h]}$ . Then, the minimum-error classification problem is formulated as

$$\min_{\{\mu_h, S_h\}_{h=1}^K} J_B(Q^c) := \pi_1 \sum_{H_0} \mathbb{P}_1[X \in S_h] + \pi_0 \sum_{H_1} \mathbb{P}_0[X \in S_h] \quad (18)$$

where  $\pi_i := \mathbb{P}[c = i]$ ,  $\mathbb{P}_i\{\cdot\} := \mathbb{P}\{\cdot|c = i\}$ , and  $H_i$  is defined as  $H_i := \{h \in \{1, \dots, K\} : Q^c = i\}$ ,  $i \in \{0, 1\}$ . In this case we can rewrite the expected distortion as

$$D = \mathbb{E}[d^b(c_X, Q^c)]$$

where  $d^b(c_x, c_\mu) = \mathbb{1}_{[c_x \neq c_\mu]}$ . Because  $d^b$  is not differentiable, using similar principles as in the case of LVQ, we can instead approximate the optimal solution by solving the minimization problem for the following distortion measure

$$d^c(x, c_x, \mu, c_\mu) = \begin{cases} d(x, \mu), & c_x = c_\mu \\ 0, & c_x \neq c_\mu \end{cases} \quad (19)$$

This particular choice for the distortion measure  $d^c$  results in important regularization properties (see Section III-E and [30]).

### E. The algorithm

The Online Deterministic Annealing (ODA) algorithm for clustering and classification is depicted in Algorithm 1. In this section we briefly discuss the properties of the algorithm, as well as the effect of the parameters used. A detailed discussion on the implementation of Alg. 1 and the effect of its parameters can be found in [30].

*Temperature Schedule.* The temperature schedule  $T_i$  plays an important role in the behavior of the algorithm. Starting at high temperature  $T_{max}$  ensures the correct operation of the algorithm. The value of  $T_{max}$  depends on the domain of the data. The stopping temperature  $T_{min}$  can be set a priori or be decided online depending on the performance of the model at each temperature level. It is common practice to use the geometric series  $T_{i+1} = \gamma T_i$ .

*Stochastic Approximation.* Regarding the stochastic approximation stepsizes, simple time-based learning rates, e.g. of the form  $\alpha_n = 1/a+bn$ , have been sufficient for fast convergence in all our experiments so far. Convergence is checked with the condition  $d_\phi(\mu_i^n, \mu_i^{n-1}) < \epsilon_c$  for a given threshold  $\epsilon_c$  that can depend on the domain of  $X$ .

*Bifurcation and Perturbations.* To every temperature level  $T_i$ , corresponds a set of effective codevectors  $\{\mu_j\}_{j=1}^{K_i}$ , which consist of the different solutions of the optimization problem (12) at  $T_i$ . Bifurcation, at  $T_i$ , is detected by maintaining a pair of perturbed codevectors  $\{\mu_j + \delta, \mu_j - \delta\}$  for each effective codevector  $\mu_j$  generated at  $T_{i-1}$ , i.e. for  $j = 1, \dots, K_{i-1}$ . Using arguments from variational calculus [32], it is easy to see that, upon convergence, the perturbed codevectors will merge if a critical temperature has not been reached, and will get separated otherwise. Therefore, the cardinality of the model is at most doubled at every temperature level. For classification, a perturbed codevector for each class is generated.

*Regularization.* Merging is detected by the condition  $d_\phi(\mu_j, \mu_i) < \epsilon_n$ , where  $\epsilon_n$  is a design parameter that acts as a regularization term for the model. Large values for  $\epsilon_n$  (compared to the support of the data  $X$ ) lead to fewer effective codevectors, while small  $\epsilon_n$  values lead to a fast growth in the model size, which is connected to overfitting. An additional regularization mechanism that comes as a natural consequence of the stochastic approximation learning rule, is the detection of idle codevectors. To see that, notice that the sequence  $\rho_i(n)$  resembles an approximation of the probability  $p(\mu_i, c_{\mu_i})$ , and whether or not they become negligible ( $\rho_i(n) < \epsilon_r$ ) is a natural criterion for removing the codevector  $\mu_i$ . The threshold  $\epsilon_r$  is a parameter that usually takes values near zero.

*Complexity.* The complexity of Alg. 1 for a fixed temperature coefficient  $T_i$  is  $O(N_{c_i}(2K_i)^2d)$ , where  $N_{c_i}$  is the number of stochastic approximation iterations needed for convergence which corresponds to the number of data samples observed,  $K_i$  is the number of codevectors of the model at temperature  $T_i$ , and  $d$  is the dimension of the input vectors, i.e.,  $x \in \mathbb{R}^d$ . Therefore, assuming a training dataset of  $N$  samples and a temperature schedule  $\{T_1 = T_{max}, T_2, \dots, T_{N_T} = T_{min}\}$ , the worst case complexity of Algorithm 1 becomes:

$$O(N_c(2\bar{K})^2d)$$

where  $N_c = \max_i \{N_{c_i}\}$  is an upper bound on the number of data samples observed until convergence at each temperature level, and

$$N_T \leq \bar{K} \leq \min \left\{ \sum_{n=0}^{N_T-1} 2^n, \sum_{n=0}^{\log_2 K_{max}} 2^n \right\} < N_T K_{max}$$

where the actual value of  $\bar{K}$  depends on the bifurcations occurred as a result of reaching critical temperatures and the effect of the regularization mechanisms described above. Note that typically  $N_c \ll N$  as a result of the stochastic approximation algorithm, and  $\bar{K} \ll N_T K_{max}$  as a result of the progressive nature of the ODA algorithm.

*Fine-Tuning.* In practice, because the convergence to the Bayes decision surface comes at the limit  $(K, T) \rightarrow (\infty, 0)$ , a fine-tuning mechanism should be designed to run on top of the proposed algorithm after  $T_{min}$ . This can be either an LVQ algorithm [49] or some other local model.

---

**Algorithm 1** Online Deterministic Annealing

---

Select Bregman divergence  $d_\phi$   
Set temperature schedule:  $T_{max}, T_{min}, \gamma$   
Decide maximum number of codevectors  $K_{max}$   
Set convergence parameters:  $\{\alpha_n\}, \epsilon_c, \epsilon_n, \epsilon_r, \delta$   
Select initial configuration  $\{\mu^i\} : c_{\mu^i} = c, \forall c \in \mathcal{C}$   
Initialize:  $K = 1, T = T_{max}$   
Initialize:  $p(\mu^i) = 1, \sigma(\mu^i) = \mu^i p(\mu^i), \forall i$   
**while**  $K < K_{max}$  **and**  $T > T_{min}$  **do**  
  Perturb  $\mu^i \leftarrow \{\mu^i + \delta, \mu^i - \delta\}, \forall i$   
  Increment  $K \leftarrow 2K$   
  Update  $p(\mu^i), \sigma(\mu^i) \leftarrow \mu^i p(\mu^i), \forall i$   
  Set  $n \leftarrow 0$   
  **repeat**  
    Observe data point  $x$  and class label  $c$   
    **for**  $i = 1, \dots, K$  **do**  
      Compute membership  $s^i = \mathbb{1}_{[c_{\mu^i}=c]}$   
      Update:  

$$p(\mu^i|x) \leftarrow \frac{p(\mu^i)e^{-\frac{d_\phi(x, \mu^i)}{T}}}{\sum_i p(\mu^i)e^{-\frac{d_\phi(x, \mu^i)}{T}}}$$
  

$$p(\mu^i) \leftarrow p(\mu^i) + \alpha_n [s^i p(\mu^i|x) - p(\mu^i)]$$
  

$$\sigma(\mu^i) \leftarrow \sigma(\mu^i) + \alpha_n [s^i x p(\mu^i|x) - \sigma(\mu^i)]$$
  

$$\mu^i \leftarrow \frac{\sigma(\mu^i)}{p(\mu^i)}$$
  
      Increment  $n \leftarrow n + 1$   
    **end for**  
  **until**  $d_\phi(\mu_n^i, \mu_{n-1}^i) < \epsilon_c, \forall i$   
  Keep effective codevectors:  
    discard  $\mu^i$  if  $d_\phi(\mu^j, \mu^i) < \epsilon_n, \forall i, j, i \neq j$   
  Remove idle codevectors:  
    discard  $\mu^i$  if  $p(\mu^i) < \epsilon_r, \forall i$   
  Update  $K, p(\mu^i), \sigma(\mu^i), \forall i$   
  Lower temperature  $T \leftarrow \gamma T$   
**end while**

---

#### IV. PROGRESSIVE LEARNING IN MULTIPLE RESOLUTIONS

As opposed to linear models or simple artificial neural networks where the forward pass is often computationally inexpensive scaling linearly with respect to the number of neurons, in prototype-based methods, every codevector has to be compared with all  $K$  of the codevectors used, resulting in a computational complexity that scales quadratically with respect to  $K$ . The progressive nature of the online deterministic annealing approach partially mitigates this problem, but as  $K$  increases, the running time of the algorithm is greatly affected. To counteract that, we impose a tree structure in the growth of the ODA model, which will also serve as a means for developing a multi-resolution online deterministic annealing learning algorithm.

##### A. Tree-Structured Online Deterministic Annealing

Tree-structured vector quantizers (TSVQ) provide computationally efficient means of compressing multivariate data. While lacking the optimality properties of full-search techniques, TSVQ are easier to implement and give rise to variable-rate codes that frequently outperform fixed-rate, full-search techniques with the same average number of bits per sample.

The progressive nature of a greedy growing tree structure aligns perfectly with the online deterministic annealing algorithm. In fact, as will be shown, ODA constructs a tree of arbitrary many children per parent node thus dropping the dependency of the number of codevectors to the number of cell splits, which is associated with the depth of the tree [50], [51]. In other words, every parent cell is split into a progressively growing number of children cells as the temperature decreases. We refer to this as a horizontal split. Once the temperature coefficient  $T$  drops below a predefined temperature threshold, then the partition is fixed and every children node will serve as a parent node that will be divided into more cells by further application of the ODA algorithm. We refer to this as a vertical split. We note that the simplicity of the splitting criterion roots in the annealing nature of ODA. The splitting criterion can even be generalized to involve additional terms such as the percentage of improvement in accuracy or distortion reduction for every temperature step.

As before, let  $X : \Omega \rightarrow S$  be a random variable. A tree-structured quantizer  $Q_\Delta : S \rightarrow S$  is defined by a set of codevectors  $M := \{\mu_h\}_{h=1}^K$  arranged in a tree structure  $\Delta$  with a single root node  $\nu_0$ . A node  $\nu_i$  represents a region  $S_{\nu_i} \subseteq S$ . It is associated with a set of codevectors  $M_{\nu_i} := \{\mu_j\}$ , where  $|M_{\nu_i}| = K_{\nu_i}$ , and a Voronoi partition  $V_{\nu_i} := \{S_j\}$  of  $S_{\nu_i}$  with respect to  $M_{\nu_i}$  and a divergence measure  $d$  (see Section III). A tree-structure is a special case of a connected, acyclic directed graph, where each node has a single parent node (except for the root node) and an arbitrary number of children nodes, that is, we do not restrict  $\Delta$  to be a binary tree. The set  $C(\nu_i)$  represents the nodes  $\{\nu_{u_j}\}$  that are the children of  $\nu_i$ , while the set  $P(\nu_j)$  represents the node  $\nu_i$  for which  $\nu_j \in C(\nu_i)$ . The level  $l \geq 0$  of a node  $\nu_h \in \Delta$  is the length of the path  $\{\nu_0, \dots, \nu_i, \nu_j, \dots, \nu_h\}$  leading from the root node  $\nu_0$  to  $\nu_h$  such that  $\nu_j \in C(\nu_i)$ . To explicitly state the level  $l$  of a node  $\nu_i$

we will write  $\nu_i^{(l)}$ . The terminal nodes  $\tilde{N} := \{\nu : C(\nu) = \emptyset\}$  are called leaves, and the union of their associated codevectors will be denoted  $\tilde{M} := \{\mu_j\}$ , where  $|\tilde{M}| = \tilde{K}$  is the number of leaf codevectors, and  $\tilde{l} := \max \left\{ l : \mu_{\nu}^{(l)} \in \tilde{M}, \forall \nu \right\} < \infty$  will denote the maximum depth of the tree. The quantizer  $Q_\Delta$  defines a hierarchical partitioning scheme for the domain  $S$ , such that for every node  $\nu_i^{(l)} \in \Delta$  associated with the region  $S_i$ , its children nodes  $\{\nu^{(l+1)} : \nu^{(l+1)} \in C(\nu_i^{(l)})\}$  are associated with the regions  $\{S_j : S_j \in V_{\nu_i}\}$  which form a Voronoi partition of  $S_{\nu_i}$  with respect to  $M_{\nu_i}$ .

After a finite number of vertical cell splits, the ODA tree  $Q_\Delta$  will have a depth  $\tilde{l} < \infty$  and a finite number  $\tilde{K} < \infty$  of leaf cells. A final application of the ODA algorithm (Alg. 1)  $\tilde{l}$  times, results, in the limit  $K \rightarrow \infty$ , in a consistent density and risk estimator, since all the assumptions needed (see [30]) carry over to the leaf cells as subsets of the original domain. We note that due to the fact that the tree-structured  $Q_\Delta$  defines a partition of  $S$ , the training of the nodes is done in parallel by doing one update of the ODA algorithm (Alg. 1) in every region  $S_i$  associated to  $\nu_i$  asynchronously, depending on what region each new observation  $X$  belongs to. As a result, depending on the density of the random variable  $X$ , some cells will be visited more often than others, which will result in some branches of the tree growing faster than others, inducing a variable-rate code that frequently outperforms fixed-rate, full-search techniques with the same average number of bits per sample. Alternatively, when learning offline using a dataset, all nodes can be trained using parallel processes, which can be utilized by multi-core computational units. Algorithm 2, presents the pseudocode for the greedy-growing Tree-Structured Online Deterministic Annealing algorithm using multiple-resolutions, as will be explained in the next section.

---

**Algorithm 2** Multi-Resolution ODA Algorithm

---

Set temperature schedule:  $\bar{T} = \{\bar{T}_{\tilde{l}}, \bar{T}_{\tilde{l}-1}, \dots, \bar{T}_0\}$ ,  $\underline{T} = \{\underline{T}_{\tilde{l}}, \underline{T}_{\tilde{l}-1}, \dots, \underline{T}_0\}$   
Initialize  $\nu_0^{(0)}$ ,  $M_{\nu_0}$ ,  $V_{\nu_0}$ .  
**repeat**  
  Observe data point  $(X, c)$   
   $w = \nu_0$ ,  $l = \tilde{l}$ ,  $x = X_{\tilde{l}}$   
  **while**  $C(w) \neq \emptyset$  **do**  
     $w = v \in C(w)$  such that  $x \in S_v$   
     $l = l - 1$   
     $x = X_l$   
  **end while**  
  Update  $M_w$  using Alg. 1 in  $S_w$  with  $(T_{max} = \bar{T}_l, T_{min} = \underline{T}_l)$   
  **if** ODA in  $S_w$  converged **and**  $l < \tilde{l}$  **then**  
    Split  $w$  to  $C(w)$  with respect to  $V_w$   
  **end if**  
**until** Convergence

---

**B. Hierarchical Learning with Multi-Resolution ODA**

The tree-growing mechanism detailed above aligns with our intuition to use more detailed information to train deeper

layers of the tree, and can be used to develop a hierarchical multi-resolution learning scheme. In the following analysis, we assume that the multi-resolution representation is defined by the subspaces  $\{V_j, j \in \mathbb{N}\}$  induced by the wavelet transform described in Section II. This analysis can be directly generalized to other hierarchical dictionaries, including the scattering transform. Consider the high-resolution representation of the input  $X_0 \in V_0 = S$  and the multi-resolution approximation defined by  $\{X_1, X_2, \dots, X_{\tilde{l}}\}$ , the projections of  $X$  to the subspaces  $\{V_1, V_2, \dots, V_{\tilde{l}}\}$ , as described in Section II. The input representations  $\{X_{\tilde{l}}, \dots, X_1, X_0\}$ , can be used to train a sequence of vector quantizers with optimal sets of codevectors  $\{M^{(\tilde{l})}, \dots, M^{(1)}, M^{(0)}\}$ , respectively, where  $M^{(l)} := \left\{ \mu_h^{(l)} \right\}_{h=1}^{K_l}$ , and  $\mu_h^{(l)} \in V_l$ . Since  $V_{\tilde{l}} \subset \dots \subset V_1 \subset V_0$ , it follows that  $X_l \in V_{\lambda < l}$ , and, as a result,  $\mu_h^{(1)} \in V_{\lambda < l}$ , for all  $l = 1, \dots, \tilde{l}$ . In other words, since the multi-resolution representation defines a sequence of spaces  $V_l \subset V_{l-1}$ , both the low-resolution representations  $X_l$  and the corresponding codevectors  $M^{(1)}$  belong to a subspace of  $V_{\lambda < l}$ , and, of course, a subspace of the original input space  $V_0$ . Because the codevectors  $\mu_h^{(l)} \in V_l$  live in a subspace of  $V_0$ , we can define the distortion  $J(M^{(l)})$  (similar to eq. 11) induced by the optimal codevectors in resolution  $l$  and measured in  $V_0$ . Similarly, we define the classification error  $L(M^{(l)}) = \pi_1(l) \sum_{H_0(l)} \mathbb{P}_1[X_0 \in S_h(l)] + \pi_0(l) \sum_{H_1(l)} \mathbb{P}_0[X_0 \in S_h(l)]$  (similar to 18), as the probability of error induced by the Voronoi partition of the codevectors  $M^{(l)}$  and measured in  $V_0$ . Because of the fact that  $V_l \subset V_0$ , it is easy to see that  $J(M^{(\lambda)}) \geq J(M^{(l)})$  and  $L(M^{(\lambda)}) \geq L(M^{(l)})$  for  $\lambda \geq l$ .

In other words, learning with progressively better approximations yields progressively better classification results, as one would expect. This fact can be exploited to reduce the computational complexity of the learning algorithm following a hierarchical architecture that mirrors the progressive attention mechanism observed in human cognition [3]–[8]. At this point, the feature space that is created through the wavelet transform (Section II), has a multi-resolution structure, while the learning module has a progressively growing tree structure. We make a fusion of the two structures by applying the using different input representations in each level of the tree, by matching the resolution ( $l$ ) to the depth level ( $\tilde{l} - l$ ) of each node. This idea was first introduced in [52] and [53]. More specifically, we start with the representation corresponding to the coarsest resolution  $X_{\tilde{l}}$  of the input (which is a projection in  $V_{\tilde{l}}$ ), and apply Alg. 1 on the region  $S_{\nu_0}$  of the root node  $\nu_0$ , until a threshold temperature is reached. At this point, the level  $l = 1$  of the tree-structured quantizer  $Q_\Delta$  has been fixed, and this qualifies as the first vertical split. The nodes  $C(\nu_0)$  are horizontally split by the application of Alg. 1 using the input representations  $X_{\tilde{l}-1}$ , and this procedure continuous until the desired distortion/accuracy level is reached, or until a stopping criterion is met, depending on the cardinality of the neurons (system resources) and the temperature of the annealing process. The multi-resolution online deterministic annealing algorithm is depicted in Alg. 2.

The resulting architecture shares similar properties with

Deep Convolutional Networks [11] and the Scattering Convolutional Networks [36], as shown in Fig. 2 and Fig. 3, and provides a general system-theoretic framework for progressive, hierarchical, and knowledge-based learning. We illustrate this framework in the block diagram of Fig. 3.

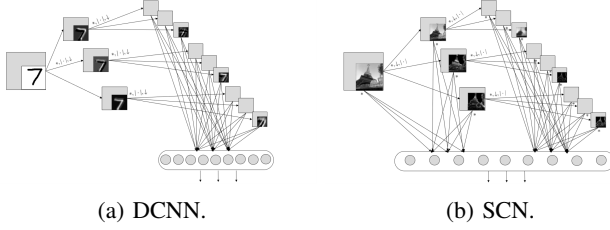


Fig. 2: The architectures of Deep Convolutional Neural Networks (DCNN) and Scattering Convolutional Networks (SCN). The arrows represent a cascade of convolution, rectifying, and downsampling operations.

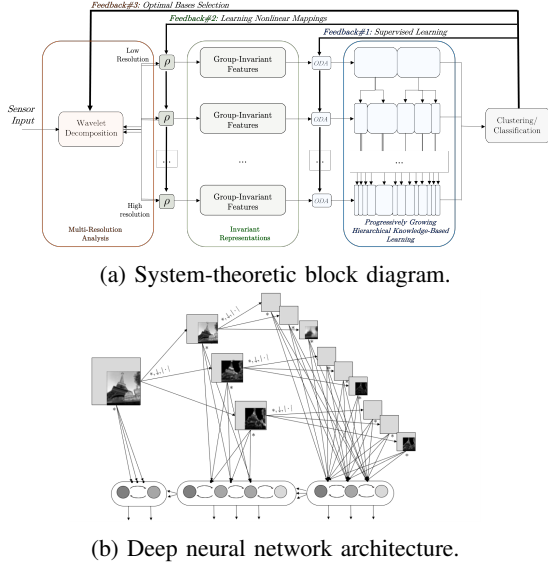


Fig. 3: Block diagram of the proposed learning architecture as a closed-loop system (a) and as a deep neural network (b). The arrows represent a cascade of convolution, rectifying, and downsampling operations.

## V. EXPERIMENTAL EVALUATION AND DISCUSSION

We illustrate the properties and evaluate the performance of the proposed learning algorithm in widely used artificial and real datasets for clustering and classification.

### A. ODA in One Resolution

We first showcase how Alg. 1 works in a simple, but illustrative, classification problem in two dimensions (Fig. 4). The underlying class distributions are shaped as concentric circles and the dataset consist of 1500 samples. Since the objective is to give a geometric illustration of how the algorithm works in the two-dimensional plane, the Euclidean distance is used. The algorithm starts at high temperature

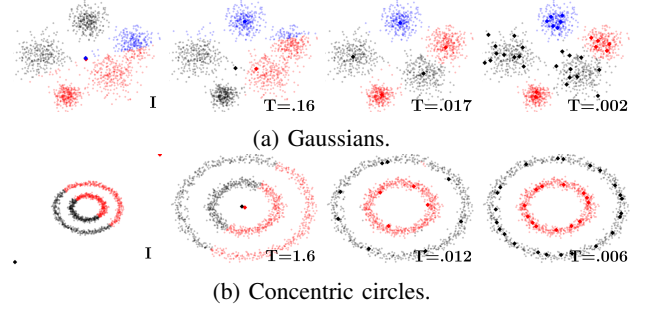


Fig. 4: Illustration of the evolution of Alg. 1 for decreasing temperature  $T$  in binary classification in 2D. (b) Showcasing robustness with respect to bad initial conditions.

with a single codevector for each class. As the temperature coefficient gradually decreases (Fig. 4, from left to right), the number of codevectors progressively increases. The accuracy of the algorithm typically increases as well. As the temperature goes to zero, the complexity of the model, i.e. the number of codevectors, rapidly increases. This may, or may not, translate to a corresponding performance boost. A single parameter – the temperature  $T$  – offers online control on this complexity-accuracy trade-off. Finally, the robustness of the proposed algorithm with respect to the initial configuration is showcased. Here the codevectors are poorly initialized outside the support of the data, which is not assumed known a priori (e.g. online observations of unknown domain). In this example the LVQ algorithm has been shown to fail [54]. In contrast, the entropy term  $H$  in the optimization objective of Alg. 1, allows for the online adaptation to the domain of the dataset and helps to prevent poor local minima. Finally, the running time of the ODA algorithm for the classification and clustering problems of the dataset in Fig. 4a is compared in Fig. 5 against state-of-the-art algorithms. All experiments were implemented on a personal computer. The reader is referred to [30] for a more detailed assessment of the ODA algorithm (Alg. 1) in both classification and clustering, as well as a discussion on the choice of the parameters and the limitations of the approach.

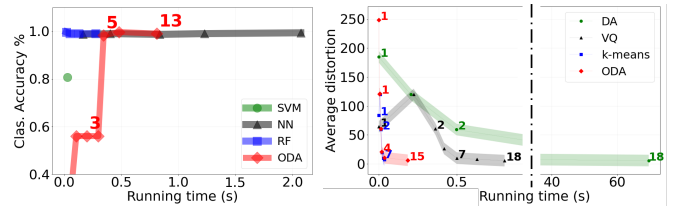


Fig. 5: Running time of the algorithms in Fig. 4a.

### B. Multi-Resolution Learning

In Fig. 6, Fig. 7, and Fig. 8, we illustrate the evolution of the multi-resolution online deterministic annealing algorithm (Alg. 2) compared to the single-resolution ODA algorithm and the tree-structured ODA algorithm, in a 2D classification problem. The accuracy of the model, the number of observations needed for convergence and the number of codevectors (neurons) used at each temperature level, are also shown.

We stress that the computational benefit of using a tree-structured architecture is significant. We remind the readers that the complexity of the ODA algorithm is  $O(N_c(2\bar{K})^2d)$ , where  $N_c$  is an upper bound on the number of data samples observed until convergence, and  $\bar{K}$  the number of effective codevectors used by the algorithm. The partition of the space in smaller sets (Voronoi regions) results in easier to solve, localized ODA problems. In particular, the size of each Voronoi set decreases in a geometric rate with respect to the depth of the tree. A decrease of similar magnitude is observed on the number  $N_c$ . If an ODA algorithm needs  $\bar{K}$  codevectors on the original domain  $S$ , a tree-structured ODA algorithm with  $\tilde{l}$  layers will require  $O(\bar{K}^{1/\tilde{l}})$  number of codevectors, assuming the same number of codevectors in each cell.

Another advantage of using a tree-structured learning module is the localization properties. The Voronoi regions shrink quickly, and allow for the use of local models, which is especially important in high-dimensional spaces. Unlike most learning models, it is possible to locate the area of the data space that presents the highest error rate and selectively split it by using local ODA. This process can be iterated until the desired error rate (or average distortion) is achieved. When using a training dataset for classification, it is often possible to force accuracy of up to 100% on the training dataset. This is similar to an over-fitted classification and regression tree (CART) [55].

However, over-fitting on the training dataset often adversely affects the generalization properties of the model, the performance on the testing dataset, and the robustness against adversarial attacks. Therefore, the progressive process of ODA becomes important in establishing a robust way to control the trade-off between performance and complexity, before you reach that limit. Finally, an important question in tree-structured learning models is the question of which cell to split next. An exhaustive search in the entire tree to find the node that presents the largest error rate is possible but is often not desired due to the large computational overhead. This is automatically answered by the multi-resolution ODA algorithm (Alg. 2) as it asynchronously updates all cells depending on the sequence of the online observations. As a result, the regions of the data space that are more densely populated with data samples are trained first, which results in a higher percentage of performance increase per cell split. We stress that this property makes the proposed algorithm completely dataset-agnostic, in the sense that it does not require the knowledge of a training dataset a priori, but instead operates completely online, i.e., using one observation at a time to update its knowledge base.

Finally, we evaluate the performance of the algorithm in image recognition, which is considered to be central to human perception and cognition. To illustrate the interpretability of the representations learned by the model, we show in Fig. 9 the weights of the neurons (codevectors) of the first two layers of a multi-resolution ODA architecture trained on the MNIST dataset [56] of hand-written digits. All 10 neurons of the first layer are shown. For the second layer, 10 of the neurons-children of each first-layer neuron are randomly selected and shown. For the first two layers, a wavelet representation of

images of  $7 \times 7$  and  $14 \times 14$  pixels was used. The testing performance for the first layer of 10 neurons is 82%, and it goes up to 89% using both layers which add up to 212 neurons. This is only using the low-resolution wavelet representation of  $14 \times 14$  pixels. Notice how different deformations of the hand-written digits are recognized by the algorithm without explicitly having to specify these transformations a priori. By studying the relationship between different codevectors that belong to the same class, it is possible to reconstruct class-invariant transformations and conserved quantities that will enable better feature extraction. We continue the learning process using two more layers based on the scattering transform provided by the ‘Kymatio’ software [45] using a spatial resolution  $J = 2$  and ‘morlet’ complex directional wavelets of four angles for the wavelet transform. We stop the process when the percentage increment in accuracy is below a certain threshold which signifies that further increase in the model complexity will likely not have a corresponding effect in the performance, and may cause over-fitting. The final architecture consists of 1,960 neurons and achieves accuracy 97.21%, in a testing dataset of 10,000 samples. As discussed above, by following this process, a knowledge representation has been built such that, if further performance boost is required, we can locate the region of the data space that should be given more emphasis. This property, in conjunction with the fact that the neurons live in the data space itself (Fig. 9), make the proposed learning architecture inherently interpretable.

### C. Source Code and Reproducibility

Code and Reproducibility: The source code is publicly available at <https://github.com/MavridisChristos/OnlineDeterministicAnnealing>.

## VI. CONCLUSION

We used principles from mathematics, system theory, and optimization to investigate the structure of a data-agnostic learning architecture that resembles the “one learning algorithm” believed to exist in the visual and auditory cortices of the human brain. Our approach consists of a closed-loop system with three main components: (i) a multi-resolution analysis pre-processor, (ii) a group-invariant feature extractor, and (iii) a progressive knowledge-based learning module, along with multi-resolution feedback loops that are used for learning. The design of (i) and (ii), is based on the well-established theory of wavelet-based multi-resolution analysis and group convolution operators. Regarding (iii), we introduced a multi-resolution extension of the Online Deterministic Annealing algorithm, a novel learning algorithm that constructs progressively growing knowledge representations. The resulting architecture shares similar properties with Deep Convolutional Networks and the Scattering Convolutional Networks but also provides a more general system-theoretic framework with some significant properties. First, it is dataset-agnostic, a term that in this case has a double meaning: it is not tailored to a specific learning task, e.g., face recognition only, and does not require the a priori knowledge of an entire dataset. In contrast, online (or real-time) observations are used to train the



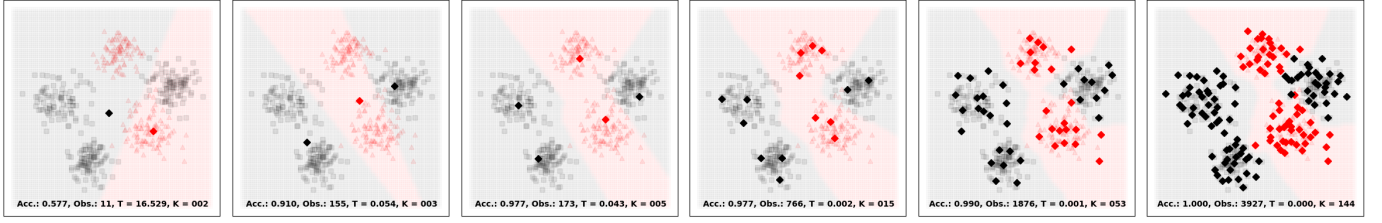


Fig. 6: Evolution of the ODA algorithm in 2D.

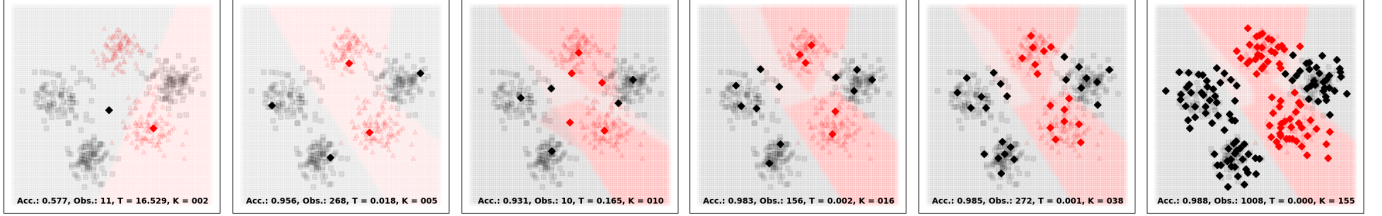


Fig. 7: Evolution of the Tree-Structured ODA algorithm in a single resolution in 2D.

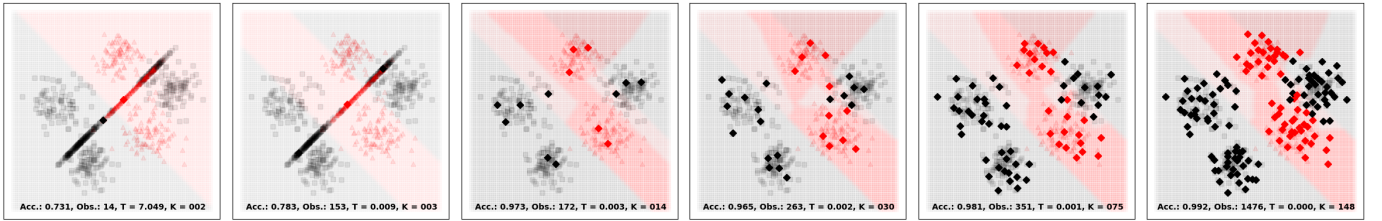


Fig. 8: Evolution of the Multi-Resolution ODA algorithm in multiple resolutions (1D and 2D). The low-resolution representations consist of the projections of the data points to the first principal component of the dataset.

algorithm. Second, it is hierarchical as a result of the multi-resolution pre-processing with the wavelet transform and the tree-structure of the learning algorithm. Third, it is memory-based, since a knowledge base, i.e., the set of codevectors representing the data space, is being built through training. In addition, it is interpretable, a term that again has a double meaning. In the case of a dataset that can be visualized by humans, the fact that the codevectors are representatives of the data space is enough to convey the information of what has been learned. Even in the general case when this is not possible, however, the proposed approach offers a structured knowledge base that can be used to localize the error-prone regions of the feature space, which leads to understanding when and why the learned model fails. This information is valuable to the designers of a learning model and can be used to incrementally improve its performance without re-training the entire model from scratch. One more property of the proposed approach is robustness with respect to initial conditions, perturbations, and adversarial attacks. This is an aftermath of the annealing optimization used to train the learning module, and the established properties of the vector quantization variants. Finally, it is progressive in the sense that the knowledge base is progressively growing, starting from very few codevectors, and adding more as needed. This interplay between compression and classification does not only help with the complexity of the model, but also with the generalization properties and with the sensitivity of

the model with respect to input noise. It also provides one of the first approaches to adaptively grow a neural network architecture, in contrast to ad-hoc experimentation on the number of neurons and number of layers to be used.

## REFERENCES

- [1] J. Bruna, A. Szlam, and Y. LeCun, "Learning stable group invariant representations with convolutional networks," *arXiv preprint arXiv:1301.3537*, 2013.
- [2] A. W. Roe, S. L. Pallas, Y. H. Kwon, and M. Sur, "Visual projections routed to the auditory pathway in ferrets: receptive fields of visual neurons in primary auditory cortex," *Journal of Neuroscience*, vol. 12, no. 9, pp. 3651–3664, 1992.
- [3] J. Sharma, A. Angelucci, and M. Sur, "Induction of visual orientation modules in auditory cortex," *Nature*, vol. 404, no. 6780, pp. 841–847, 2000.
- [4] P. Taylor, J. Hobbs, J. Burrone, and H. Siegelmann, "The global landscape of cognition: hierarchical aggregation as an organizational principle of human cortical networks and functions," *Scientific reports*, vol. 5, no. 1, pp. 1–18, 2015.
- [5] M. Riesenhuber and T. Poggio, "Hierarchical models of object recognition in cortex," *Nature neuroscience*, vol. 2, no. 11, pp. 1019–1025, 1999.
- [6] M. Ito and H. Komatsu, "Representation of angles embedded within contour stimuli in area v2 of macaque monkeys," *Journal of Neuroscience*, vol. 24, no. 13, pp. 3313–3324, 2004.
- [7] H. L. Read, J. A. Winer, and C. E. Schreiner, "Functional architecture of auditory cortex," *Current opinion in neurobiology*, vol. 12, no. 4, pp. 433–440, 2002.
- [8] T. Chi, P. Ru, and S. A. Shamma, "Multiresolution spectrotemporal analysis of complex sounds," *The Journal of the Acoustical Society of America*, vol. 118, no. 2, pp. 887–906, 2005.
- [9] G. A. Carpenter and S. Grossberg, "Adaptive resonance theory," 2010.



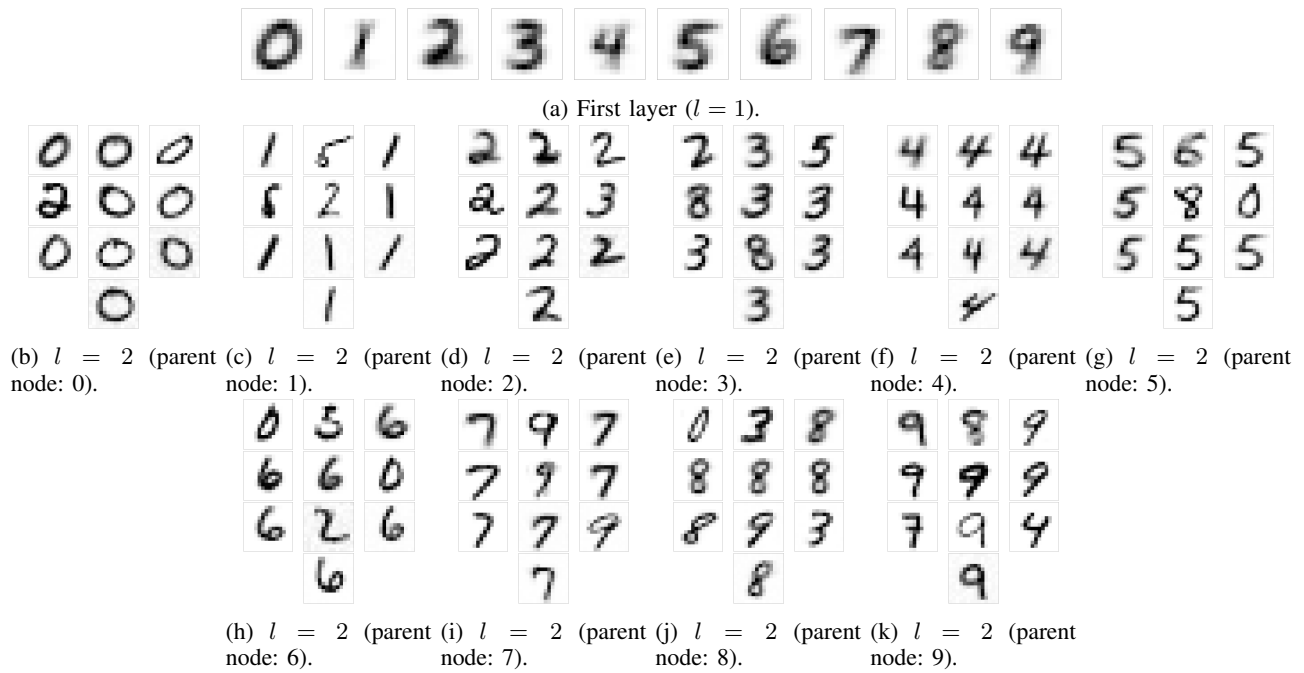


Fig. 9: Learned representations of the first two layers a multi-resolution Online Deterministic Annealing algorithm trained on the MNIST dataset.

- [10] T. Poggio, T. A. Poggio, and F. Anselmi, *Visual cortex and deep networks: learning invariant representations*. MIT Press, 2016.
- [11] Y. LeCun, Y. Bengio, and G. Hinton, “Deep learning,” *nature*, vol. 521, no. 7553, pp. 436–444, 2015.
- [12] G. E. Hinton, S. Osindero, and Y.-W. Teh, “A fast learning algorithm for deep belief nets,” *Neural computation*, vol. 18, no. 7, pp. 1527–1554, 2006.
- [13] A. Krizhevsky, I. Sutskever, and G. E. Hinton, “Imagenet classification with deep convolutional neural networks,” in *Advances in neural information processing systems*, 2012, pp. 1097–1105.
- [14] H. Lee, R. Grosse, R. Ranganath, and A. Y. Ng, “Convolutional deep belief networks for scalable unsupervised learning of hierarchical representations,” in *Proceedings of the 26th annual international conference on machine learning*, 2009, pp. 609–616.
- [15] M. I. Jordan, “Artificial intelligence—the revolution hasn’t happened yet,” *Harvard Data Science Review*, vol. 1, no. 1, 7 2019, <https://hdsr.mitpress.mit.edu/pub/wot7mkc1>. [Online]. Available: <https://hdsr.mitpress.mit.edu/pub/wot7mkc1>
- [16] N. C. Thompson, K. Greenewald, K. Lee, and G. F. Manso, “The computational limits of deep learning,” *arXiv preprint arXiv:2007.05558*, 2020.
- [17] E. Strubell, A. Ganesh, and A. McCallum, “Energy and policy considerations for deep learning in nlp,” *arXiv preprint arXiv:1906.02243*, 2019.
- [18] C. Szegedy, W. Zaremba, I. Sutskever, J. Bruna, D. Erhan, I. Goodfellow, and R. Fergus, “Intriguing properties of neural networks,” *arXiv preprint arXiv:1312.6199*, 2013.
- [19] N. Carlini and D. Wagner, “Towards evaluating the robustness of neural networks,” in *2017 IEEE Symposium on Security and Privacy (SP)*. IEEE, 2017, pp. 39–57.
- [20] A. Madry, A. Makelov, L. Schmidt, D. Tsipras, and A. Vladu, “Towards deep learning models resistant to adversarial attacks,” *arXiv preprint arXiv:1706.06083*, 2017.
- [21] V. Schwag, A. N. Bhagoji, L. Song, C. Sitawarin, D. Cullina, M. Chiang, and P. Mittal, “Analyzing the robustness of open-world machine learning,” in *Proceedings of the 12th ACM Workshop on Artificial Intelligence and Security*, 2019, pp. 105–116.
- [22] C. G. Northcutt, A. Athalye, and J. Mueller, “Pervasive label errors in test sets destabilize machine learning benchmarks,” *arXiv preprint arXiv:2103.14749*, 2021.
- [23] T. Poggio, A. Banburski, and Q. Liao, “Theoretical issues in deep networks,” *Proceedings of the National Academy of Sciences*, 2020.
- [24] S. Mallat, “Understanding deep convolutional networks,” *Philosophical Transactions of the Royal Society A: Mathematical, Physical and Engineering Sciences*, vol. 374, no. 2065, p. 20150203, 2016.
- [25] R. Vidal, J. Bruna, R. Giryes, and S. Soatto, “Mathematics of deep learning,” *arXiv preprint arXiv:1712.04741*, 2017.
- [26] C. Liu, L. Zhu, and M. Belkin, “Toward a theory of optimization for over-parameterized systems of non-linear equations: the lessons of deep learning,” *arXiv preprint arXiv:2003.00307*, 2020.
- [27] L. Von Melchner, S. L. Pallas, and M. Sur, “Visual behaviour mediated by retinal projections directed to the auditory pathway,” *Nature*, vol. 404, no. 6780, pp. 871–876, 2000.
- [28] L. Thaler, S. R. Arnott, and M. A. Goodale, “Neural correlates of natural human echolocation in early and late blind echolocation experts,” *PLoS one*, vol. 6, no. 5, p. e20162, 2011.
- [29] S. Mallat, “Group invariant scattering,” *Communications on Pure and Applied Mathematics*, vol. 65, no. 10, pp. 1331–1398, 2012.
- [30] C. Mavridis and J. Baras, “Online deterministic annealing for classification and clustering,” *arXiv preprint arXiv:2102.05836*, 2021.
- [31] S. Saralajew, L. Holdijk, M. Rees, and T. Villmann, “Robustness of generalized learning vector quantization models against adversarial attacks,” in *International Workshop on Self-Organizing Maps*. Springer, 2019, pp. 189–199.
- [32] K. Rose, “Deterministic annealing for clustering, compression, classification, regression, and related optimization problems,” *Proceedings of the IEEE*, vol. 86, no. 11, pp. 2210–2239, 1998.
- [33] V. S. Borkar, *Stochastic approximation: a dynamical systems viewpoint*. Springer, 2009, vol. 48.
- [34] A. Banerjee, S. Merugu, I. S. Dhillon, and J. Ghosh, “Clustering with bregman divergences,” *Journal of machine learning research*, vol. 6, no. Oct, pp. 1705–1749, 2005.
- [35] T. Villmann, S. Haase, F.-M. Schleif, B. Hammer, and M. Biehl, “The mathematics of divergence based online learning in vector quantization,” in *IAPR Workshop on Artificial Neural Networks in Pattern Recognition*. Springer, 2010, pp. 108–119.
- [36] J. Bruna and S. Mallat, “Invariant scattering convolution networks,” *IEEE transactions on pattern analysis and machine intelligence*, vol. 35, no. 8, pp. 1872–1886, 2013.
- [37] J. Zhao, M. Mathieu, and Y. LeCun, “Energy-based generative adversarial network,” *arXiv preprint arXiv:1609.03126*, 2016.
- [38] Y. LeCun, “The next frontier in ai: Unsupervised learning,” <https://www.youtube.com/watch?v=IbjF5VjniVE>, 2016.
- [39] F. Anselmi, J. Z. Leibo, L. Rosasco, J. Mutch, A. Tacchetti, and T. Pog-

gio, “Unsupervised learning of invariant representations,” *Theoretical Computer Science*, vol. 633, pp. 112–121, 2016.

- [40] S. Geman, “Compositionality in vision,” *The grammar of vision: probabilistic grammar-based models for visual scene understanding and object categorization*, 2007.
- [41] F. Anselmi, L. Rosasco, C. Tan, and T. Poggio, “Deep convolutional networks are hierarchical kernel machines,” *arXiv preprint arXiv:1508.01084*, 2015.
- [42] A. L. Yuille and C. Liu, “Deep nets: What have they ever done for vision?” *arXiv preprint arXiv:1805.04025*, 2018.
- [43] S. G. Mallat, “A theory for multiresolution signal decomposition: the wavelet representation,” *IEEE transactions on pattern analysis and machine intelligence*, vol. 11, no. 7, pp. 674–693, 1989.
- [44] S. Mallat, *A wavelet tour of signal processing*. Elsevier, 1999.
- [45] M. Andreux, T. Angles, G. Exarchakis, R. Leonarduzzi, G. Rochette, L. Thiry, J. Zarka, S. Mallat, J. Andén, E. Belilovsky, J. Bruna, V. Lostanlen, M. J. Hirn, E. Oyallon, S. Zhang, C. Cella, and M. Eickenberg, “Kymatio: Scattering transforms in python,” 2019.
- [46] Y. Zhuang and J. S. Baras, “Optimal wavelet basis selection for signal representation,” in *Wavelet Applications*, vol. 2242. International Society for Optics and Photonics, 1994, pp. 200–211.
- [47] C. N. Mavridis and J. S. Baras, “Convergence of stochastic vector quantization and learning vector quantization with bregman divergences,” *IFAC-PapersOnLine*, vol. 53, no. 2, pp. 2214–2219, 2020.
- [48] E. T. Jaynes, “Information theory and statistical mechanics,” *Physical review*, vol. 106, no. 4, p. 620, 1957.
- [49] T. Kohonen, *Learning Vector Quantization*. Berlin, Heidelberg: Springer Berlin Heidelberg, 1995, pp. 175–189.
- [50] E. A. Riskin and R. M. Gray, “A greedy tree growing algorithm for the design of variable rate vector quantizers (image compression),” *IEEE Transactions on Signal Processing*, vol. 39, no. 11, pp. 2500–2507, 1991.
- [51] A. B. Nobel and R. A. Olshen, “Termination and continuity of greedy growing for tree-structured vector quantizers,” *IEEE Transactions on Information Theory*, vol. 42, no. 1, pp. 191–205, 1996.
- [52] J. S. Baras and S. I. Wolk, “Efficient organization of large ship radar databases using wavelets and structured vector quantization,” in *Proceedings of 27th Asilomar Conference on Signals, Systems and Computers*. IEEE, 1993, pp. 491–498.
- [53] —, “Wavelet-based progressive classification of high-range resolution radar returns,” in *Wavelet Applications*, H. H. Szu, Ed., vol. 2242, International Society for Optics and Photonics. SPIE, 1994, pp. 967 – 977. [Online]. Available: <https://doi.org/10.1117/12.170034>
- [54] J. S. Baras and A. LaVigna, “Convergence of a neural network classifier,” in *Advances in Neural Information Processing Systems*, 1991, pp. 839–845.
- [55] L. Breiman, “Random forests,” *Machine learning*, vol. 45, no. 1, pp. 5–32, 2001.
- [56] Y. LeCun, L. Bottou, Y. Bengio, and P. Haffner, “Gradient-based learning applied to document recognition,” *Proceedings of the IEEE*, vol. 86, no. 11, pp. 2278–2324, 1998.



**Christos N. Mavridis** (M’20) received the Diploma degree in electrical and computer engineering from the National Technical University of Athens, Greece, in 2017, and the M.S. and Ph.D. degrees in electrical and computer engineering at the University of Maryland, College Park, MD, USA, in 2021. His research interests include learning theory, stochastic optimization, systems and control theory, multi-agent systems, and robotics.

He has worked as a researcher at the Department of Electrical and Computer Engineering at the University of Maryland, College Park, MD, USA, and as a research intern for the Math and Algorithms Research Group at Nokia Bell Labs, NJ, USA, and the System Sciences Lab at Xerox Palo Alto Research Center (PARC), CA, USA.

Dr. Mavridis is an IEEE member, and a member of the Institute for Systems Research (ISR) and the Autonomy, Robotics and Cognition (ARC) Lab. He received the Ann G. Wylie Dissertation Fellowship in 2021, and the A. James Clark School of Engineering Distinguished Graduate Fellowship, Outstanding Graduate Research Assistant Award, and Future Faculty Fellowship, in 2017, 2020, and 2021, respectively. He has been a finalist in the Qualcomm Innovation Fellowship US, San Diego, CA, 2018, and he has received the Best Student Paper Award (1st place) in the IEEE International Conference on Intelligent Transportation Systems (ITSC), 2021.



**John S. Baras** (LF’13) received the Diploma degree in electrical and mechanical engineering from the National Technical University of Athens, Athens, Greece, in 1970, and the M.S. and Ph.D. degrees in applied mathematics from Harvard University, Cambridge, MA, USA, in 1971 and 1973, respectively.

He is a Distinguished University Professor and holds the Lockheed Martin Chair in Systems Engineering, with the Department of Electrical and Computer Engineering and the Institute for Systems Research (ISR), at the University of Maryland College Park. From 1985 to 1991, he was the Founding Director of the ISR. Since 1992, he has been the Director of the Maryland Center for Hybrid Networks (HYNET), which he co-founded. His research interests include systems and control, optimization, communication networks, applied mathematics, machine learning, artificial intelligence, signal processing, robotics, computing systems, security, trust, systems biology, healthcare systems, model-based systems engineering.

Dr. Baras is a Fellow of IEEE (Life), SIAM, AAAS, NAI, IFAC, AMS, AIAA, Member of the National Academy of Inventors and a Foreign Member of the Royal Swedish Academy of Engineering Sciences. Major honors include the 1980 George Axelby Award from the IEEE Control Systems Society, the 2006 Leonard Abraham Prize from the IEEE Communications Society, the 2017 IEEE Simon Ramo Medal, the 2017 AACC Richard E. Bellman Control Heritage Award, the 2018 AIAA Aerospace Communications Award. In 2016 he was inducted in the A. J. Clark School of Engineering Innovation Hall of Fame. In 2018 he was awarded a Doctorate Honoris Causa by his alma mater the National Technical University of Athens, Greece.